Published in final edited form as:
Cancer Res. 2014 December 15; 74(24): 7534–7545. doi:10.1158/0008-5472.CAN-14-2650.

Identification of ATR-Chk1 pathway inhibitors that selectively target p53-deficient cells without directly suppressing ATR catalytic activity

Masaoki Kawasumi[1,a], **James E. Bradner**[2,3,4], **Nicola Tolliday**[2], **Renee Thibodeau**[1], **Heather Sloan**[1], **Kay M. Brummond**[5], and **Paul Nghiem**[1,6,a]

[1]Division of Dermatology, Department of Medicine, University of Washington, Seattle, Washington, 98109

[2]The Broad Institute of MIT and Harvard, Cambridge, Massachusetts, 02142

[3]Department of Medical Oncology, Dana-Farber Cancer Institute, Boston, Massachusetts, 02115

[4]Department of Medicine, Harvard Medical School, Boston, Massachusetts, 02115

[5]University of Pittsburgh Center for Chemical Methodologies and Library Development, Pittsburgh, Pennsylvania, 15260

[6]Clinical Research Division, Fred Hutchinson Cancer Research Center, Seattle, Washington, 98109

Abstract

Resistance to DNA-damaging chemotherapy is a barrier to effective treatment that appears to be augmented by p53 functional deficiency in many cancers. In p53-deficient cells where the G_1/S checkpoint is compromised, cell viability after DNA damage relies upon intact intra-S and G_2/M checkpoints mediated by the ATR and Chk1 kinases. Thus, a logical rationale to sensitize p53-deficient cancers to DNA-damaging chemotherapy is through the use of ATP-competitive inhibitors of ATR or Chk1. To discover small molecules that may act on uncharacterized components of the ATR pathway, we performed a phenotype-based screen of 9,195 compounds for their ability to inhibit hydroxyurea-induced phosphorylation of Ser345 on Chk1, known to be a critical ATR substrate. This effort led to the identification of four small-molecule compounds, three of which were derived from known bioactive library (anthothecol, dihydrocelastryl, and erysolin) and one of which was a novel synthetic compound termed MARPIN. These compounds all inhibited ATR-selective phosphorylation and sensitized p53-deficient cancer cells to DNA-damaging agents *in vitro* and *in vivo*. Notably, these compounds did not inhibit ATR catalytic activity *in vitro*, unlike typical ATP-competitive inhibitors, but acted in a mechanistically distinct manner to disable ATR-Chk1 function. Our results highlight a set of novel molecular probes to

[a]Correspondence: Masaoki Kawasumi, MD, PhD, Division of Dermatology, Department of Medicine, University of Washington, 850 Republican Street, Brotman 242, Seattle, Washington 98109, USA, Phone: 206-221-4594; Fax: 206-221-4364; kawasumi@uw.edu; Paul Nghiem, MD, PhD, Division of Dermatology, Department of Medicine, University of Washington, 850 Republican Street, Brotman 242, Seattle, Washington 98109, USA, Phone: 206-221-2632; Fax: 206-221-4364; pnghiem@uw.edu.

Competing Financial Interests Statement: The authors declare no competing financial interests.

further elucidate druggable mechanisms to improve cancer therapeutic responses produced by DNA-damaging drugs.

Keywords

Small-molecule inhibitors; chemosensitization; high-content screen; ATR-Chk1 pathway; cell cycle checkpoint

Introduction

Genotoxic stresses including ionizing radiation, ultraviolet (UV) irradiation, and many chemotherapeutic agents elicit DNA damage checkpoints that promote cell-cycle arrest and DNA repair (1). ATM (ataxia telangiectasia mutated) and ATR (ataxia telangiectasia and Rad3-related) are key protein kinases that sense DNA damage and phosphorylate their downstream targets to activate DNA damage checkpoints. Ionizing radiation and doxorubicin cause DNA double strand breaks and primarily activate the ATM-Chk2-p53 pathway. UV and hydroxyurea cause stalled replication forks and primarily activate the ATR-Chk1 pathway. However, there is extensive crosstalk between these two pathways (2). The resultant signaling is affected by diverse factors including types and doses of stress as well as timing. Most types of genotoxic stress activate both pathways to some degree.

Targeting DNA damage checkpoints could be beneficial to cancer treatment (3-5). In normal cells, DNA-damaging agents activate ATM and/or ATR pathways that mediate G_1/S, intra-S, and G_2/M checkpoints to arrest cell cycle progression and allow extra time for DNA repair. Many cancers are deficient in the G_1/S checkpoint, including those with defective p53 (6,7). This results in reliance on later checkpoints for DNA repair and cell survival, including the ATR pathway. If the ATR pathway is inhibited in G_1 checkpoint-deficient cells in the presence of DNA damage, cells will not elicit cell cycle arrest for DNA repair, leading to cancer cell death (8). Thus, inhibiting the ATR pathway has been an appealing strategy to selectively sensitize p53-deficient cells to chemotherapeutic agents that damage DNA (3,4,9).

Because ATR inhibition can sensitize cancer cells to DNA-damaging agents (8,10,11), inhibitors that target the ATR-Chk1 pathway are of great interest for cancer therapy, and some Chk1 inhibitors have entered clinical trials (4,5,9). Caffeine is widely used as a non-selective ATM/ATR inhibitor (IC_{50} of 200 μM for ATM; IC_{50} of 1,100 μM for ATR) (12), but more selective and potent ATR inhibitors have been long sought to better understand DNA damage response pathways and to use as chemosensitizers in combination with chemotherapeutic agents (13). Recently, schisandrin B, a dibenzocyclooctadiene derivative isolated from an herb, has been identified as a potent ATR-selective inhibitor (IC_{50} of 7.25 μM for ATR) (14). Additionally, aminopyrazine derivatives, Compound 45 (IC_{50} of 0.012 μM for ATR) (15) and VE-821 (IC_{50} of 0.026 μM for ATR) (16), have been identified as highly potent ATR-selective inhibitors. These compounds sensitized cancer cells to cisplatin, while sparing normal cells (15,16), further supporting the potential utility of ATR inhibition to sensitize cancer cells to death.

The mechanism of ATR activation is complex, requiring recruitment of more than 10 proteins at sites of DNA damage for optimal kinase activation (17). Briefly, a replication fork stalls at DNA lesions, while helicases continue to separate DNA strands, generating single-stranded DNA (ssDNA) coated with RPA (17). Multiple proteins including the 9-1-1 complex, TopBP1, and Claspin are then recruited to RPA-coated ssDNA. Thus, not only ATR kinase but also a handful of known proteins involved in ATR pathway activation could be targets for suppression of the ATR pathway. Most compounds that target this pathway are believed to act as ATP-competitive inhibitors of ATR kinase activity, such as caffeine, schisandrin B, or VE-821. Compounds that target other components of the ATR pathway are few in number and typically affect nonspecific processes such as protein chaperones and stability. For example, Hsp90 inhibitors (geldanamycin and 17-allylamino-17-demethoxygeldanamycin (17-AAG)) deplete Chk1 and hence block ATR pathway function, as well as many other targets (18,19).

A chemical genetic screen is a powerful approach to discover small-molecule compounds that perturb cellular processes and elucidate biological systems (20,21). Small molecules that suppress the ATR-Chk1 pathway without inhibiting ATR could be identified through pathway-targeted screening. Such compounds could uncover previously unknown but druggable targets in signaling pathways or reveal known targets for which no small-molecule inhibitors have been identified. To discover novel DNA damage response inhibitors that target the ATR pathway, we performed cell-based, high-content screening of small-molecule compounds. Following biological assays for validation, we found 4 novel small-molecule compounds that inhibit the ATR-Chk1 pathway. Importantly, these four compounds did not directly inhibit ATR kinase catalytic activity *in vitro* but had chemosensitization effects, especially in p53-deficient cells *in vitro*. One compound, dihydrocelastryl, was also tested in a xenograft model and showed selective inhibition of p53-deficient tumor growth *in vivo*. Identification of these mechanistically distinct inhibitors of DNA damage checkpoints allows their use as probes to further elucidate checkpoint function.

Materials and Methods

Cell lines and culture conditions

HeLa and 293T cells were obtained from American Type Culture Collection (ATCC), authenticated through short tandem repeat (STR) profiling by ATCC, and cultured in Dulbecco's Modified Eagle Medium (DMEM; #11995; Invitrogen) supplemented with 10% Heat-Inactivated Fetal Bovine Serum (FBS; Invitrogen) and 1% Penicillin-Streptomycin (PS; Invitrogen). HCT116 $p53^{+/+}$ cells and the isogenic $p53^{-/-}$ cells were gifts from Dr. Bert Vogelstein (Johns Hopkins University) (22) and cultured in McCoy's 5A Medium (#16600; Invitrogen) supplemented with 10% FBS and 1% PS. p53 expression in HCT116 $p53^{+/+}$ and $p53^{-/-}$ cells was validated by Western blot analyses. Upon receipt of all cell lines, frozen stocks were made at low passage and thawed for short-term culture (less than 3 months). All cells were maintained at 37 °C in a humidified atmosphere of 5% CO_2.

Small-molecule screening by automated cell imaging

Screening was performed at the Broad Institute of MIT and Harvard using its small-molecule libraries, comprising known bioactive and novel synthetic compounds. Primary screen data were deposited to ChemBank (http://chembank.broadinstitute.org) under the project name "DNADamageImagingScreen". HeLa cells (4,000 cells per well) were plated onto 384-well flat clear bottom black polystyrene tissue culture treated microplates (#3712; Corning) and incubated at 37 °C overnight in a humidified atmosphere of 5% CO_2. Compound mixture of hydroxyurea (HU) and a test compound for cell treatment was prepared in a separate 384-well plate: 100 mM hydroxyurea was diluted with cell culture medium (DMEM supplemented with 10% FBS and 1% PS) to a final concentration of 3 mM in 45 μl medium in each well, and a single small-molecule compound was added to each well by 100 nl pin-transfer (CyBio) of a compound stock solution in DMSO. Culture medium was aspirated, and 45 μl of compound mixture was added to each well that also contained 5 μl of residual culture medium (total 50 μl per well). Because the average compound concentration of stock solution was 10 mM in DMSO, the final compound concentration for cell treatment was 20 μM in test wells (final DMSO 0.2%). Cells were incubated with 3 mM hydroxyurea and a single small-molecule compound in each well at 37 °C for 2 h in a humidified atmosphere of 5% CO_2. For immunofluorescence, cells were fixed by adding 15 μl/well of 16% paraformaldehyde (formaldehyde) aqueous solution (#15710; Electron Microscopy Sciences) to 50 μl medium in each well (final 4% formaldehyde) and incubating at 4 °C overnight. Fixed cells were treated with 2N HCl (50 μl/well) for 10 min at room temperature. Cells were washed twice with 50 μl/well of Tris-buffered saline (TBS; 50 mM Tris, 150 mM NaCl, pH 7.4) and treated with 50 μl/well of TBS supplemented with 0.5% Triton X-100 for 15 min at room temperature. Cells were washed with 50 μl/well of TBS and treated with 50 μl/well of TBS supplemented with 0.1% sodium borohydride (#452882; Sigma-Aldrich) for 5 min at room temperature. Cells were washed twice with 50 μl/well of TBS and treated with 50 μl/well of TBS supplemented with 3% bovine serum albumin (BSA; A9647; Sigma-Aldrich) [3% BSA-TBS] for 10 min at room temperature. Cells were incubated with 20 μl/well of 1:150 dilution of anti-phospho-Chk1 (pChk1 – Ser345) [133D3] rabbit monoclonal antibody (#2348; Cell Signaling Technology) in 3% BSA-TBS at 4 °C overnight. Cells were washed with 50 μl/well of 3% BSA-TBS and incubated with 20 μl/well of 1:150 dilution of Alexa Fluor 488 goat anti-rabbit IgG antibody (A-11034; Invitrogen) in 3% BSA-TBS for 1.5 h at room temperature. Cells were washed with 50 μl/well of 3% BSA-TBS and incubated with 20 μl/well of 1:10 dilution of VECTASHIELD Mounting Medium with DAPI (1.5 μg/ml DAPI) (H-1200; Vector Laboratories) in 3% BSA-TBS for 30 min at room temperature. Cells were washed twice with 50 μl/well of 3% BSA-TBS and twice with 50 μl/well of TBS. Immunofluorescent images of cells stained with anti-pChk1 antibody and DAPI in each well were acquired by automated fluorescence microscopy using DAPI and FITC filters (ImageXpress; Molecular Devices) and analyzed by MetaXpress (Molecular Devices). To detect pChk1 signals only from nuclei and eliminate background signals from cytoplasm and the surface of cell culture wells, pChk1 nuclear signal intensity in each well was quantitated within all nuclei of HeLa cells (determined by DAPI-positive areas). To normalize cell number differences among wells of screening plates, average pChk1 nuclear signal intensity for one test compound in each well was calculated by dividing pChk1 nuclear signal

intensity from all nuclei in each well by the number of nuclei (DAPI-positive areas). For hit compound selection, the average of pChk1 intensities among all 384 wells of each plate (whole plate average intensity) was defined as 100% (because most compounds had a little or no effect on HU-induced Chk1 phosphorylation), and compounds whose average pChk1 nuclear signal intensities were <85% were chosen for follow-up.

Supplementary Materials and Methods include: chemicals, siRNA transfection, treatment with DNA-damaging agents, Western blot analyses, flow cytometry analyses, *in vitro* ATR kinase assay, cell viability assay, human tumor xenografts in athymic nude mice, and statistical analyses.

Results

A cell-based screen for novel ATR pathway inhibitors

To discover DNA damage response inhibitors that suppress the ATR pathway and to gain insight into replication checkpoint signaling, we performed a cell-based, high-content screen of small-molecule libraries using an automated cell imaging platform. The specific small-molecule screen involved detection of hydroxyurea (HU)-induced phosphorylation of Chk1 at Ser345, a downstream target of ATR, as an indicator for ATR pathway activation (23,24). HU inhibits DNA synthesis and stalls replication forks. This replication stress activates the ATR pathway, leading to phosphorylation of Chk1. In this screen, HeLa cells were plated onto 384-well plates and treated with HU and a single small-molecule compound in each well (Fig. 1A). HeLa cells were selected for this cell imaging assay, because this cell type demonstrated a robust signaling response and remained adherent during washing steps required for immunofluorescence. Cells were stained with anti-phospho-Chk1 (pChk1 − Ser345) antibody and DAPI for nuclear staining, and the immunofluorescent images of cells in each well were acquired by automated fluorescence microscopy. Subsequently, the acquired images were analyzed to quantitate pChk1 signal intensities within nuclei that were defined by DAPI-positive areas. Compounds that suppressed HU-induced Chk1 phosphorylation were selected as putative ATR pathway inhibitors.

Using this approach, HU-induced pChk1 was reliably detected as a significant increase in pChk1 nuclear signal intensity (middle bar in Fig. 1B) compared to untreated cells (left bar). Addition of 3 mM caffeine (right bar) suppressed HU-induced phosphorylation of Chk1 to 85% of pChk1 intensity of HU-treated cells. This effect on pChk1 signal intensity in cells was consistent with Western blot results using the same pChk1 antibody (Fig. 1B), although untreated cells showed no pChk1 signal in a Western blot. Despite relatively high non-specific background immunofluorescence in the microscopy assay, cell imaging at the single nucleus level was reliable in detecting phospho-Chk1 signals in a high-throughput manner.

Figure 1C shows a representative result of one 384-well plate from the primary screen. Average pChk1 intensity of 384 wells was set to 100% (whole plate average shown as a solid horizontal line), presuming that the majority of compounds were not ATR pathway inhibitors and thus the whole plate average was virtually the same as the level of pChk1 induced by HU alone. Compounds that decreased the nuclear pChk1 signal below 85% (dotted horizontal line) of the whole plate average were more potent than 3 mM caffeine,

and thus were selected for follow-up. From the example plate shown in Figure 1C, dihydrocelastryl was selected for follow-up while teniposide, thiram, and bleomycin showed high levels of pChk1 intensity (Fig. 1C). These latter three compounds are indeed known DNA-damaging agents that activate DNA damage response pathways, suggesting this assay could appropriately detect both activating and inhibitory compounds.

In a secondary screen, we performed dose-response experiments in triplicate by the same automated cell imaging assay (Fig. 2A). Increasing doses of caffeine inhibited HU-induced pChk1 as a positive control. The four novel compounds (anthothecol, dihydrocelastryl, erysolin, and MARPIN: 'ATM and ATR pathway inhibitor') also inhibited phosphorylation in a dose-dependent manner, all of which were significantly more potent than caffeine.

Because we performed a small-molecule screen detecting HU-induced pChk1, we needed to exclude the possibility that these novel compounds could be merely modulators of HU-induced signaling, not ATR pathway inhibitors. In a tertiary screen, we performed Western blot analyses to validate the inhibitory effects of novel compounds on pChk1 induced by two mechanistically distinct ATR pathway activators: hydroxyurea (HU; acts by nucleotide depletion) and ultraviolet irradiation (UV; acts by generating polymerase-blocking thymine dimers). HU-induced pChk1 was inhibited by these novel compounds in a dose-dependent manner (Fig. 2B) as was UV-induced pChk1 (Fig. 2C). These findings confirmed that these compounds are indeed ATR pathway inhibitors, not merely modulators of HU-induced signaling.

In total, we screened 9,195 compounds from two distinct small-molecule libraries, comprising known bioactive and novel synthetic compounds (Fig. 2D). The average compound concentration in this cell-based screen was 20 μM following pin transfer of the compounds into test wells. Test compounds that did not show dose-dependent inhibition of HU-induced pChk1 in the secondary and tertiary screens were eliminated from further investigation. After these screens by cell imaging and Western blot analyses, we eventually identified 4 novel ATR pathway inhibitors from 9,195 compounds.

Chemical structures of these novel ATR pathway inhibitors and caffeine are shown in Figure 2E. The four novel ATR pathway inhibitors were structurally different from each other and from caffeine. Anthothecol, dihydrocelastryl, and erysolin were derived from libraries of known bioactive compounds and are commercially available. The fourth inhibitor, identified from a diversity-oriented synthetic library, was named MARPIN (ATM and ATR pathway inhibitor) based on its ability to inhibit both the ATM and ATR pathways, as determined in subsequent experiments. MARPIN's chemical name is methyl (1R,6aR)-2-benzoyl-1-(4-fluorobenzyl)-6-methylene-5-oxo-1,2,3,5,6,6a-hexahydrocyclopenta[c]pyrrole-1-carboxylate [ChemBank ID 1965360, PubChem Substance ID 11253916, PubChem Compound ID 3247230]. To the best of our knowledge, none of these 4 compounds have been previously reported to be DNA damage response pathway inhibitors. The hit rate from the known bioactive compounds library (0.12%) was much higher than that of the synthetic library (0.015%). This difference in hit rates supports the idea that the known bioactive compounds are heavily biased towards biologically active compounds and that the cellular activities of these agents have not yet been exhaustively described.

All four novel ATR pathway inhibitors suppressed HU-induced pChk1 at concentrations below 30 μM in the immunofluorescence imaging assays, while caffeine required 3,000 μM for the same degree of pChk1 inhibition (Fig. 2E). Thus, the novel compounds were at least 100 times more potent than caffeine for ATR pathway inhibition in cells.

Novel ATR pathway inhibitors abrogate G_2/M checkpoint induced by ionizing radiation

A pivotal function of DNA damage response kinases is to elicit cell cycle checkpoint signaling and stop cell cycle progression, allowing time for DNA repair (4). To determine whether novel inhibitors functionally suppress cell cycle arrest, the effect of these compounds on the ionizing radiation (IR)-induced G_2/M checkpoint was assessed by measuring the percentage of cells positive for phospho-Histone H3 (Ser10) with 4N DNA content as an indicator of mitosis. After 2 h, 2 Gy of IR decreased the percentage of mitotic cells from 2.2% to 0.1% (Fig. 3A), indicating that IR activated the G_2/M checkpoint and inhibited mitotic entry. Known inhibitors of ATM and/or ATR abrogated the IR-induced G_2/M checkpoint, including caffeine (dual ATM/ATR inhibitor), KU-55933 (ATM-selective inhibitor), and VE-821 (ATR-selective inhibitor) (Fig. 3). These data suggest that the IR-induced G_2/M checkpoint is mediated via both ATM and ATR, consistent with prior studies (25,26). Furthermore, all four novel ATR pathway inhibitors we discovered abrogated IR-induced G_2/M checkpoint in a dose-dependent manner (Fig. 3), supporting that these inhibitors functionally block the induction of cell cycle arrest, a pivotal role for DNA damage response pathways.

Novel ATR pathway inhibitors do not directly suppress ATR catalytic activity

To investigate whether novel compounds directly inhibit the catalytic activity of ATR kinase, we performed *in vitro* ATR kinase assays using immunopurified ATR proteins (Fig. 4). Known nonspecific ATR inhibitors, caffeine (12) and wortmannin (27), suppressed ATR kinase activity, validating the ATR kinase assay. However, none of the four novel compounds suppressed ATR kinase activity *in vitro* even at far higher concentrations of these compounds than were required to inhibit HU-induced pChk1 in cells. These results suggest that the novel inhibitors are mechanistically distinct from caffeine in their mode of suppressing ATR signaling in cells.

Inhibition of ATR- and ATM-selective phosphorylation by novel compounds

To examine whether these novel inhibitors suppress ATR- or ATM-dependent phosphorylation events or both, we carefully selected conditions under which signaling is predominantly dependent on ATR or ATM, as there is often crosstalk between these two pathways (2). To this end, we used siRNA against ATR or ATM to determine the extent to which a signaling event was dependent on either of these kinases. This survey examined approximately 700 phospho-specific events under various conditions or time-points: 3 different cell types (HeLa, 293T, and HCT116), 5 DNA-damaging agents (HU, UV, IR, bleomycin, and doxorubicin), 3 doses of each agent, 5 time points, and 6 different phosphorylation sites on 4 DNA damage response proteins (Chk1 (Ser317 and Ser345), p53 (Ser15 and Ser20), Chk2 (Thr68), and ATM (Ser1981)) for their dependence on either of these kinases. We ultimately identified HU-induced phospho-Chk1 (Ser345) and phospho-

p53 (Ser15) at 2 h in 293T cells as the most ATR-selective phosphorylation events (Fig. 5A). The most ATM-selective signaling event was phospho-Chk2 (Thr68) induced by low dose (2 Gy) of IR at an early time point (15 min) in HCT116 $p53^{+/+}$ cells (Fig. 5B). We then used these optimized, pathway-selective conditions to test the extent to which the novel inhibitors suppressed signaling via the ATR and ATM pathways. All 4 compounds inhibited ATR-selective phosphorylation events (HU-induced phospho-Chk1 and phospho-p53) in a dose-dependent manner (Fig. 5C). Erysolin and MARPIN inhibited IR-induced phospho-Chk2 in a dose-dependent manner, but anthothecol or dihydrocelastryl did not inhibit this ATM-selective phosphorylation event (Fig. 5D). Taken together, all 4 compounds are ATR pathway inhibitors, two of which also have ability to suppress the ATM pathway at an early time point.

Novel ATR pathway inhibitors sensitize p53-deficient cells to DNA damage

G_1 checkpoint-deficient cells, particularly those deficient in p53 function, are resistant to DNA-damaging agents but can be sensitized by ATR (8) or Chk1 (28,29) inhibition. Therefore, we tested whether these novel ATR pathway inhibitors would also sensitize cancer cells to DNA damage. To investigate whether these ATR pathway inhibitors can overcome the chemoresistance of p53-deficient cells, we examined cell viability after treating cells with combinations of DNA-damaging agents with novel ATR pathway inhibitors. We used HCT116 cells (human colorectal cancer cell lines), because the isogenic $p53^{-/-}$ cells are available (22), and we can readily compare p53 wild-type ($p53^{+/+}$) and p53-deficient ($p53^{-/-}$) cells.

First, we investigated whether novel ATR pathway inhibitors sensitize cancer cells to cisplatin, a DNA crosslinker. Cisplatin was selected because other studies have shown that it synergizes effectively with ATR inhibition in killing cancer cells (11,30). In p53 wild-type cells, cisplatin alone (10 μM) decreased cell viability (to 75%), while p53-deficient cells were resistant to cisplatin (92% cell viability) (Fig. 6A). Cisplatin plus anthothecol (1 μM) showed a marked synergistic decrease in cell viability, especially in p53-deficient cells (15% cell viability).

Because ATR inhibition potentiates the effects of various classes of chemotherapeutic drugs (11,31), we also examined whether these novel ATR pathway inhibitors sensitize cancer cells to camptothecin, a Topoisomerase I poison that results in S phase slowing. Camptothecin alone (120 nM) decreased cell viability, especially in p53 wild-type cells (53% cell viability) (Fig. 6B), but p53-deficient cells were relatively resistant to camptothecin (73% cell viability). Although 1 μM dihydrocelastryl had no effect in either cell type if given alone, it fully reversed the camptothecin-resistant phenotype of p53-deficient cells (73% cell viability with camptothecin alone vs. 21% when dihydrocelastryl was added).

To precisely examine whether novel ATR pathway inhibitors show synergistic effects on decreasing cell viability in combination with DNA-damaging agents, we extensively tested various concentrations of compounds (Supplementary Fig. S1). These cell viability data were used to calculate synergistic effects on decreasing cell viability (see example in Fig. 6C). All novel ATR pathway inhibitors and caffeine showed significant synergistic lethality

with cisplatin (Fig. 6D) and camptothecin (Fig. 6E), especially in p53-deficient cells. In contrast, an ATM-selective inhibitor KU-55933 (32,33) showed a modest synergistic effect on cisplatin treatment, implying that ATR inhibition plays a more important role in sensitizing cancer cells to cisplatin. These results demonstrate that chemoresistant p53-deficient cells can be sensitized by these novel ATR pathway inhibitors. As single agents, these compounds showed modest cytotoxicity in HCT116 cancer cells at concentrations which caused synergistic sensitization effects in HCT116 cells (Supplementary Fig. S1) but no cytotoxicity in normal cells (primary human keratinocytes at 24 h).

The doses of novel inhibitors required for effective synergistic lethality at 48 h (1-8 μM; Fig. 6) were ∼8- to 60-fold lower than doses required for inhibition of HU-induced pChk1 at 2 h (15-60 μM; Fig. 5C). To verify that such very low doses of novel inhibitors that were used for synergistic lethality experiments can suppress cisplatin-induced pChk1, we used flow cytometry (a highly sensitive assay) to detect pChk1 status. Flow cytometry-based measurement of pChk1 was validated by detecting the inhibitory effect of VE-821 (established ATR-selective inhibitor) on HU-induced pChk1 (Supplementary Fig. S2A and S2B). Cisplatin induced phosphorylation of Chk1 at Ser345 predominantly in S phase, although pChk1 induction by 10 μM cisplatin was subtle, compared to pChk1 induced by 3 mM HU (Supplementary Fig. S2). At the very low doses that showed synergistic lethality, all four novel ATR pathway inhibitors weakly but reproducibly suppressed cisplatin-induced pChk1 (Supplementary Fig. S2D). This suggests that low levels of ATR-Chk1 pathway inhibition are sufficient to sensitize cells to DNA-damaging agents after 48 h, exhibiting effective synergistic lethality.

A novel ATR pathway inhibitor synergizes with cisplatin to suppress p53-deficient tumor growth *in vivo*

Because novel ATR pathway inhibitors indeed sensitized cancer cells to DNA damage *in vitro*, we investigated the *in vivo* anti-tumor activity of a novel ATR pathway inhibitor and its synergistic effect with cisplatin in a xenograft model. We selected dihydrocelastryl for testing its *in vivo* efficacy, because it was commercially available and preliminary *in vivo* data suggested efficacy at a concentration at which the compound could be dissolved. We employed a subcutaneous tumor xenograft mouse model implanted with the human colon carcinoma cell line (HCT116) which we had also used for cell viability studies. This HCT116 xenograft model has been widely used to study anti-tumor activity of small-molecule compounds (34). We used both HCT116 p53-intact ($p53^{+/+}$) cells and the isogenic p53-null ($p53^{-/-}$) cells in order to elucidate p53 dependency on eliminating cancer cells. Because high doses (4 or 8 mg/kg/day) of cisplatin in our injection schedule resulted in severe body weight loss, we used 2 mg/kg/day of cisplatin that did not cause loss of body weight. Dihydrocelastryl at 0.1 mg/kg/day also did not cause loss of body weight. Cisplatin alone inhibited growth of $p53^{+/+}$ tumors (52% tumor volume compared with vehicle treatment), and the addition of dihydrocelastryl had no effect (Fig. 7A). Importantly, $p53^{-/-}$ tumors were relatively resistant to cisplatin (85% tumor volume compared with vehicle treatment), and dihydrocelastryl sensitized $p53^{-/-}$ tumors to cisplatin, suppressing tumor volume to 60% (Fig. 7B). Thus, dihydrocelastryl demonstrated synergistic suppression of chemoresistant $p53^{-/-}$ tumor growth *in vivo*.

Discussion

Because of potential chemotherapeutic (sensitization of chemoresistant cells to death) (3,4) and chemopreventive (skin cancer prevention) (35) implications, ATR pathway inhibitors have long been sought. Caffeine has been widely used as an ATM/ATR inhibitor, but caffeine requires millimolar levels to inhibit ATR and has several other targets (12,36). Previous attempts to discover novel DNA damage response inhibitors have focused on finding better ATP-competitive inhibitors of kinases in this pathway. In the present study, we employed a phenotype-based screening approach to identify ATR pathway inhibitors, potentially mechanistically distinct from typical ATP-competitive kinase inhibitors. Because the ATR activation mechanism is complex and requires multiple proteins to be recruited to damaged DNA, any of these components of the ATR pathway could potentially be a target of the identified small-molecule inhibitors. Specifically, unlike traditional biochemical screening, this phenotype-based approach allowed us to discover novel ATR pathway inhibitors that are bioactive and do not act as direct ATR kinase catalytic inhibitors.

Mutations of p53 are the most common genetic abnormality in human cancers. The prevalence of p53 dysfunction is ∼50% in major human cancers including lung, colon, and skin cancers (6). p53-deficient cells are resistant to DNA-damaging agents (37), and there is thus a need to sensitize p53-deficient cells for effective cancer therapy. Because ATR inhibition can sensitize G_1 checkpoint-deficient cells to DNA-damaging agents (8), we investigated the chemosensitization abilities of novel ATR pathway inhibitors in the present study. The ATR pathway inhibitors demonstrated synergistic effects on cancer cell killing in p53-deficient cells. Despite the fact that these compounds did not directly inhibit ATR kinase catalytic activity, the compounds blocked ATR pathway function and promoted sensitization of drug-resistant p53-deficient cells. Previous studies demonstrated that loss of ATM sensitizes p53-deficient cells to camptothecin, but not cisplatin (38), while ATR inhibition can sensitize cancer cells to both camptothecin (31) and cisplatin (11). In particular, p53-deficient cells are preferentially sensitized to cisplatin by ATR inhibition (39). The inhibitors we describe here sensitized p53-deficient cells to both cisplatin and camptothecin. This wide range of chemosensitization effects of the ATR pathway inhibitors is potentially advantageous to cancer therapeutic applications.

Certain barriers often block translation of a given small-molecule compound to the *in vivo* setting even if the compound has desired *in vitro* effects. These barriers include solubility of the compound, *in vivo* stability, drug delivery to tumors, and toxicity (40). To investigate the *in vivo* characteristics of a novel ATR pathway inhibitor, we tested one compound, dihydrocelastryl, using a xenograft model. Dihydrocelastryl was selected for xenograft experiments, because it showed strong chemosensitization for $p53^{-/-}$ cells in cell viability study and in an *in vivo* pilot study. Dihydrocelastryl overcame these barriers and synergistically sensitized p53-deficient tumors in combination with cisplatin *in vivo* without severe body weight loss or any other overt health concerns. This synergistic effect on anti-tumor efficacy *in vivo* is meaningful for reducing the dose of cisplatin in order to minimize undesired toxic effects of chemotherapeutic agents, because higher doses of cisplatin (4 or 8 mg/kg/day) were toxic to mice in this experimental setting, inducing cachexia. Thus, ATR

pathway inhibitors have the potential to improve the efficacy of existing chemotherapeutic agents that cause DNA damage.

Three of the novel ATR pathway inhibitors that we discovered were from a library of known bioactive compounds. Anthothecol is a limonoid of *Khaya anthotheca* (the mahogany family Meliaceae) and has antimalarial activity (41). Dihydrocelastryl is structurally similar to celastrol, a triterpene extracted from the root bark of the Chinese medicine “Thunder of God Vine”. Celastrol is a potent proteasome inhibitor and suppresses human prostate cancer growth in nude mice (42). Erysolin is structurally similar to sulforaphane, an isothiocyanate that has antimicrobial activity and shows cancer preventive effects (43). Sulforaphane is abundant in broccoli sprouts. Sulforaphane and erysolin induce detoxification enzymes (44). The induction of detoxification enzymes may be a significant component of the anticarcinogenic action of broccoli. Importantly, based on PubMed/literature searches, we were unable to find prior studies which suggest that any of these compounds may act as inhibitors of DNA damage checkpoint function.

Because these novel compounds inhibited the ATR pathway without directly affecting ATR kinase catalytic activity, it is plausible that the compounds may inhibit a mediator protein involved in this signaling pathway. Previous studies showed that ATM and ATR functions could be suppressed by downregulating a protein required for their signaling such as BRCA1 (45), protein phosphatase 5 (46,47), or Timeless (48,49). Thus, it is possible that the ATR pathway inhibitors target a non-kinase component of the ATM/ATR pathways to suppress signal transduction. Further investigation to elucidate direct molecular targets of these novel ATR pathway inhibitors is ongoing, with a particular focus on target identification for MARPIN using structure-activity relationship studies and MARPIN-immobilized beads to pull down relevant binding proteins (50).

In conclusion, a cell-based phenotypic screen yielded novel ATR-Chk1 pathway inhibitors that are mechanistically distinct from typical kinase inhibitors and effectively sensitize p53-deficient cells not only *in vitro* but also in an *in vivo* xenograft model. This phenotype-based approach has the advantage that it can identify bioactive small-molecule compounds that could target any aspect of the ATR pathway, rather than focusing only on ATR kinase catalytic activity. Importantly, these compounds that are not ATR catalytic inhibitors will be useful as probes to better understand DNA damage response pathways. Detailed characterization of the mechanisms of action will further elucidate ATR pathway function in response to various types of DNA damage, and may identify novel druggable proteins for cancer prevention and therapy.

Supplementary Material

Refer to Web version on PubMed Central for supplementary material.

Acknowledgments

We thank Dr. Bert Vogelstein (Johns Hopkins University) for the gift of HCT116 $p53^{+/+}$ and the isogenic $p53^{-/-}$ cells. Allan Conney, PhD, passed away in 2013. We are deeply grateful for the inspirational role that Dr. Conney played in this study.

Grant Support: This work was supported by the National Institutes of Health (R01-AR049832 to P.N.), a Dermatology Foundation Career Development Award (to M.K.), and the Michael Piepkorn Endowment for Dermatology Research at University of Washington.

References

1. Ciccia A, Elledge SJ. The DNA damage response: making it safe to play with knives. Mol Cell. 2010; 40:179–204. [PubMed: 20965415]
2. Helt CE, Cliby WA, Keng PC, Bambara RA, O'Reilly MA. Ataxia telangiectasia mutated (ATM) and ATM and Rad3-related protein exhibit selective target specificities in response to different forms of DNA damage. J Biol Chem. 2005; 280:1186–92. [PubMed: 15533933]
3. Zhou BB, Bartek J. Targeting the checkpoint kinases: chemosensitization versus chemoprotection. Nat Rev Cancer. 2004; 4:216–25. [PubMed: 14993903]
4. Lapenna S, Giordano A. Cell cycle kinases as therapeutic targets for cancer. Nat Rev Drug Discov. 2009; 8:547–66. [PubMed: 19568282]
5. Furgason JM, Bahassi el M. Targeting DNA repair mechanisms in cancer. Pharmacol Ther. 2013; 137:298–308. [PubMed: 23107892]
6. Greenblatt MS, Bennett WP, Hollstein M, Harris CC. Mutations in the p53 tumor suppressor gene: clues to cancer etiology and molecular pathogenesis. Cancer Res. 1994; 54:4855–78. [PubMed: 8069852]
7. Paulovich AG, Toczyski DP, Hartwell LH. When checkpoints fail. Cell. 1997; 88:315–21. [PubMed: 9039258]
8. Nghiem P, Park PK, Kim Y, Vaziri C, Schreiber SL. ATR inhibition selectively sensitizes G1 checkpoint-deficient cells to lethal premature chromatin condensation. Proc Natl Acad Sci U S A. 2001; 98:9092–7. [PubMed: 11481475]
9. Chen T, Stephens PA, Middleton FK, Curtin NJ. Targeting the S and G2 checkpoint to treat cancer. Drug Discov Today. 2012; 17:194–202. [PubMed: 22192883]
10. Cliby WA, Roberts CJ, Cimprich KA, Stringer CM, Lamb JR, Schreiber SL, et al. Overexpression of a kinase-inactive ATR protein causes sensitivity to DNA-damaging agents and defects in cell cycle checkpoints. EMBO J. 1998; 17:159–69. [PubMed: 9427750]
11. Wilsker D, Bunz F. Loss of ataxia telangiectasia mutated- and Rad3-related function potentiates the effects of chemotherapeutic drugs on cancer cell survival. Mol Cancer Ther. 2007; 6:1406–13. [PubMed: 17431119]
12. Sarkaria JN, Busby EC, Tibbetts RS, Roos P, Taya Y, Karnitz LM, et al. Inhibition of ATM and ATR kinase activities by the radiosensitizing agent, caffeine. Cancer Res. 1999; 59:4375–82. [PubMed: 10485486]
13. Wagner JM, Kaufmann SH. Prospects for the use of ATR inhibitors to treat cancer. Pharmaceuticals. 2010; 3:1311–34.
14. Nishida H, Tatewaki N, Nakajima Y, Magara T, Ko KM, Hamamori Y, et al. Inhibition of ATR protein kinase activity by schisandrin B in DNA damage response. Nucleic Acids Res. 2009; 37:5678–89. [PubMed: 19625493]
15. Charrier JD, Durrant SJ, Golec JM, Kay DP, Knegtel RM, MacCormick S, et al. Discovery of potent and selective inhibitors of ataxia telangiectasia mutated and Rad3 related (ATR) protein kinase as potential anticancer agents. J Med Chem. 2011; 54:2320–30. [PubMed: 21413798]
16. Reaper PM, Griffiths MR, Long JM, Charrier JD, Maccormick S, Charlton PA, et al. Selective killing of ATM- or p53-deficient cancer cells through inhibition of ATR. Nat Chem Biol. 2011; 7:428–30. [PubMed: 21490603]
17. Cimprich KA, Cortez D. ATR: an essential regulator of genome integrity. Nat Rev Mol Cell Biol. 2008; 9:616–27. [PubMed: 18594563]
18. Arlander SJ, Eapen AK, Vroman BT, McDonald RJ, Toft DO, Karnitz LM. Hsp90 inhibition depletes Chk1 and sensitizes tumor cells to replication stress. J Biol Chem. 2003; 278:52572–7. [PubMed: 14570880]

19. Sugimoto K, Sasaki M, Isobe Y, Tsutsui M, Suto H, Ando J, et al. Hsp90-inhibitor geldanamycin abrogates G2 arrest in p53-negative leukemia cell lines through the depletion of Chk1. Oncogene. 2008; 27:3091–101. [PubMed: 18071310]
20. Kawasumi M, Nghiem P. Chemical genetics: elucidating biological systems with small-molecule compounds. J Invest Dermatol. 2007; 127:1577–84. [PubMed: 17568801]
21. Mitchison TJ. Small-molecule screening and profiling by using automated microscopy. Chembiochem. 2005; 6:33–9. [PubMed: 15568196]
22. Bunz F, Dutriaux A, Lengauer C, Waldman T, Zhou S, Brown JP, et al. Requirement for p53 and p21 to sustain G2 arrest after DNA damage. Science. 1998; 282:1497–501. [PubMed: 9822382]
23. Liu Q, Guntuku S, Cui XS, Matsuoka S, Cortez D, Tamai K, et al. Chk1 is an essential kinase that is regulated by Atr and required for the G(2)/M DNA damage checkpoint. Genes Dev. 2000; 14:1448–59. [PubMed: 10859164]
24. Zhao H, Piwnica-Worms H. ATR-mediated checkpoint pathways regulate phosphorylation and activation of human Chk1. Mol Cell Biol. 2001; 21:4129–39. [PubMed: 11390642]
25. Brown EJ, Baltimore D. Essential and dispensable roles of ATR in cell cycle arrest and genome maintenance. Genes Dev. 2003; 17:615–28. [PubMed: 12629044]
26. Cuadrado M, Martinez-Pastor B, Murga M, Toledo LI, Gutierrez-Martinez P, Lopez E, et al. ATM regulates ATR chromatin loading in response to DNA double-strand breaks. J Exp Med. 2006; 203:297–303. [PubMed: 16461339]
27. Sarkaria JN, Tibbetts RS, Busby EC, Kennedy AP, Hill DE, Abraham RT. Inhibition of phosphoinositide 3-kinase related kinases by the radiosensitizing agent wortmannin. Cancer Res. 1998; 58:4375–82. [PubMed: 9766667]
28. Wang Q, Fan S, Eastman A, Worland PJ, Sausville EA, O'Connor PM. UCN-01: a potent abrogator of G2 checkpoint function in cancer cells with disrupted p53. J Natl Cancer Inst. 1996; 88:956–65. [PubMed: 8667426]
29. Ma CX, Cai S, Li S, Ryan CE, Guo Z, Schaiff WT, et al. Targeting Chk1 in p53-deficient triple-negative breast cancer is therapeutically beneficial in human-in-mouse tumor models. J Clin Invest. 2012; 122:1541–52. [PubMed: 22446188]
30. Arora S, Bisanz KM, Peralta LA, Basu GD, Choudhary A, Tibes R, et al. RNAi screening of the kinome identifies modulators of cisplatin response in ovarian cancer cells. Gynecol Oncol. 2010; 118:220–7. [PubMed: 20722101]
31. Cliby WA, Lewis KA, Lilly KK, Kaufmann SH. S phase and G2 arrests induced by topoisomerase I poisons are dependent on ATR kinase function. J Biol Chem. 2002; 277:1599–606. [PubMed: 11700302]
32. Hickson I, Zhao Y, Richardson CJ, Green SJ, Martin NM, Orr AI, et al. Identification and characterization of a novel and specific inhibitor of the ataxia-telangiectasia mutated kinase ATM. Cancer Res. 2004; 64:9152–9. [PubMed: 15604286]
33. Knight ZA, Gonzalez B, Feldman ME, Zunder ER, Goldenberg DD, Williams O, et al. A pharmacological map of the PI3-K family defines a role for p110alpha in insulin signaling. Cell. 2006; 125:733–47. [PubMed: 16647110]
34. Buzzai M, Jones RG, Amaravadi RK, Lum JJ, DeBerardinis RJ, Zhao F, et al. Systemic treatment with the antidiabetic drug metformin selectively impairs p53-deficient tumor cell growth. Cancer Res. 2007; 67:6745–52. [PubMed: 17638885]
35. Kawasumi M, Lemos B, Bradner JE, Thibodeau R, Kim YS, Schmidt M, et al. Protection from UV-induced skin carcinogenesis by genetic inhibition of the ataxia telangiectasia and Rad3-related (ATR) kinase. Proc Natl Acad Sci U S A. 2011; 108:13716–21. [PubMed: 21844338]
36. Sabisz M, Skladanowski A. Modulation of cellular response to anticancer treatment by caffeine: inhibition of cell cycle checkpoints, DNA repair and more. Curr Pharm Biotechnol. 2008; 9:325–36. [PubMed: 18691092]
37. Bunz F, Hwang PM, Torrance C, Waldman T, Zhang Y, Dillehay L, et al. Disruption of p53 in human cancer cells alters the responses to therapeutic agents. J Clin Invest. 1999; 104:263–9. [PubMed: 10430607]

38. Fedier A, Schlamminger M, Schwarz VA, Haller U, Howell SB, Fink D. Loss of atm sensitises p53-deficient cells to topoisomerase poisons and antimetabolites. Ann Oncol. 2003; 14:938–45. [PubMed: 12796033]
39. Sangster-Guity N, Conrad BH, Papadopoulos N, Bunz F. ATR mediates cisplatin resistance in a p53 genotype-specific manner. Oncogene. 2011; 30:2526–33. [PubMed: 21258400]
40. Lin JH, Lu AY. Role of pharmacokinetics and metabolism in drug discovery and development. Pharmacol Rev. 1997; 49:403–49. [PubMed: 9443165]
41. Lee SE, Kim MR, Kim JH, Takeoka GR, Kim TW, Park BS. Antimalarial activity of anthothecol derived from Khaya anthotheca (Meliaceae). Phytomedicine. 2008; 15:533–5. [PubMed: 17913482]
42. Yang H, Chen D, Cui QC, Yuan X, Dou QP. Celastrol, a triterpene extracted from the Chinese "Thunder of God Vine," is a potent proteasome inhibitor and suppresses human prostate cancer growth in nude mice. Cancer Res. 2006; 66:4758–65. [PubMed: 16651429]
43. Fahey JW, Haristoy X, Dolan PM, Kensler TW, Scholtus I, Stephenson KK, et al. Sulforaphane inhibits extracellular, intracellular, and antibiotic-resistant strains of Helicobacter pylori and prevents benzo[a]pyrene-induced stomach tumors. Proc Natl Acad Sci U S A. 2002; 99:7610–5. [PubMed: 12032331]
44. Zhang Y, Talalay P, Cho CG, Posner GH. A major inducer of anticarcinogenic protective enzymes from broccoli: isolation and elucidation of structure. Proc Natl Acad Sci U S A. 1992; 89:2399–403. [PubMed: 1549603]
45. Foray N, Marot D, Gabriel A, Randrianarison V, Carr AM, Perricaudet M, et al. A subset of ATM- and ATR-dependent phosphorylation events requires the BRCA1 protein. EMBO J. 2003; 22:2860–71. [PubMed: 12773400]
46. Ali A, Zhang J, Bao S, Liu I, Otterness D, Dean NM, et al. Requirement of protein phosphatase 5 in DNA-damage-induced ATM activation. Genes Dev. 2004; 18:249–54. [PubMed: 14871926]
47. Zhang J, Bao S, Furumai R, Kucera KS, Ali A, Dean NM, et al. Protein phosphatase 5 is required for ATR-mediated checkpoint activation. Mol Cell Biol. 2005; 25:9910–9. [PubMed: 16260606]
48. Unsal-Kacmaz K, Mullen TE, Kaufmann WK, Sancar A. Coupling of human circadian and cell cycles by the timeless protein. Mol Cell Biol. 2005; 25:3109–16. [PubMed: 15798197]
49. Yang X, Wood PA, Hrushesky WJ. Mammalian TIMELESS is required for ATM-dependent CHK2 activation and G2/M checkpoint control. J Biol Chem. 2010; 285:3030–4. [PubMed: 19996108]
50. Huryn DM, Brodsky JL, Brummond KM, Chambers PG, Eyer B, Ireland AW, et al. Chemical methodology as a source of small-molecule checkpoint inhibitors and heat shock protein 70 (Hsp70) modulators. Proc Natl Acad Sci U S A. 2011; 108:6757–62. [PubMed: 21502524]

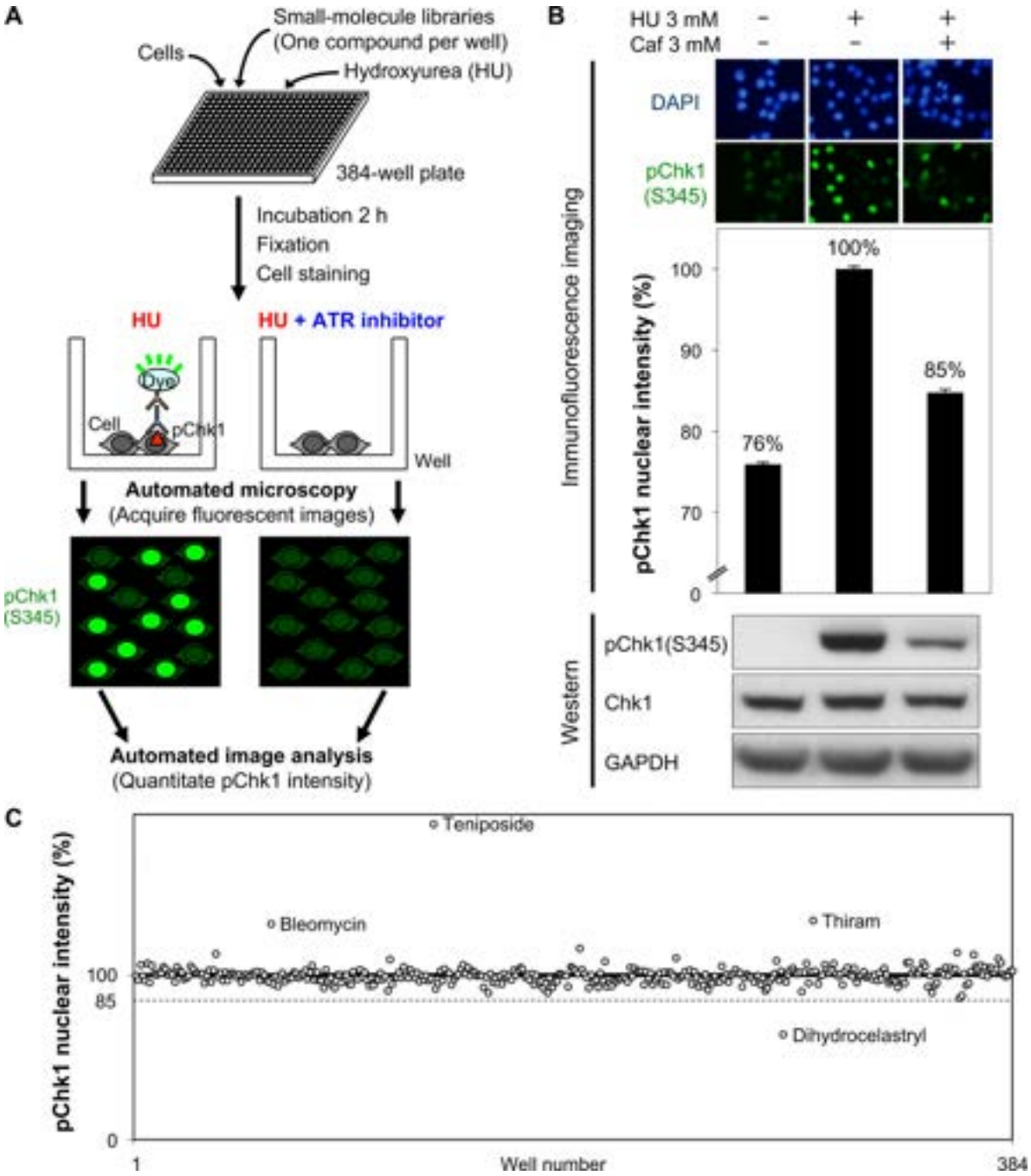

Figure 1. A high-content imaging screen for discovery of ATR pathway inhibitors

(**A**) Schematic of a cell-based, phenotypic screen for compounds that inhibit hydroxyurea (HU)-induced phosphorylation of Chk1 (pChk1) at Ser345.

(**B**) Chk1 phosphorylation was quantitated within the nuclei of HeLa cells (determined by DAPI-positive areas) following 2 h incubation with hydroxyurea (HU) and/or caffeine (Caf) as indicated. Representative cell images are shown (top panel). The mean of pChk1 nuclear intensity was calculated among 128 wells for each of three conditions (middle panel). Error bars indicate standard error of the mean (n = 128 wells). The pChk1 signal in HU-treated

wells was defined as 100%. Background immunofluorescence signal in this assay was 76% in the absence of HU. Western blot analysis using clarified cell lysates indicates that this relatively high immunofluorescence background is not due to baseline Chk1 phosphorylation (lower panel).

(**C**) Representative data from one 384-well plate from the primary screen. Each dot indicates the average pChk1 nuclear signal intensity (pChk1 signal normalized across all nuclei) from one well in which cells were treated with hydroxyurea plus one test compound. The average of pChk1 intensities among all 384 wells of each plate (solid horizontal line) was defined as 100%. Most compounds had a little or no effect on HU-induced Chk1 phosphorylation. The threshold for selecting compounds that inhibited Chk1 phosphorylation was set to 85% (dotted horizontal line) or below, because 3 mM caffeine (effectively inhibits ATR at this concentration) typically suppressed HU-induced Chk1 phosphorylation to 85%.

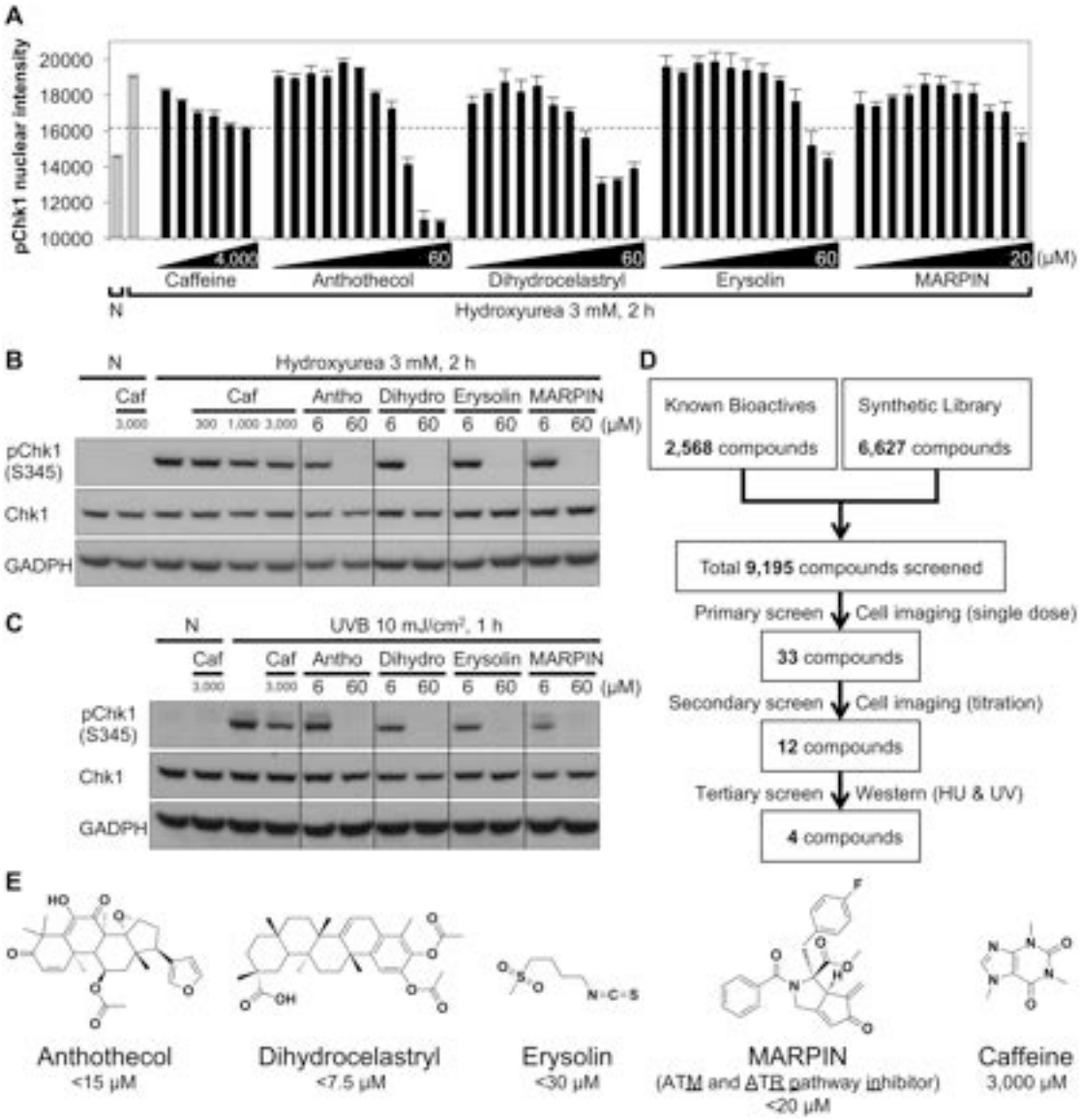

Figure 2. Validation studies of compounds identified in the initial screen

(**A**) Secondary screen by automated cell imaging for dose responses. HeLa cells were mock treated (N: no hydroxyurea (1st grey bar)), or treated with hydroxyurea (HU) alone (2nd grey bar) or with various concentrations of a test compound for 2 h (black bars). Cells were stained with anti-phospho-Chk1 (pChk1 − Ser345) antibody and DAPI. pChk1 signal was quantitated by automated cell imaging as in Figure 1. Two-fold serial dilutions of compounds were tested in triplicate, and mean of pChk1 nuclear intensity is shown. The highest concentration (μM) used for a compound is indicated within the black triangles. The dotted horizontal line indicates the ability of 3 mM caffeine to inhibit HU-induced pChk1. Error bars indicate standard error of the mean.

(**B**) Tertiary screen by Western blot analysis of HU-induced pChk1. HeLa cells were mock treated (N: no HU) or treated with HU and various concentrations of a test compound for 2 h.

(**C**) Inhibition of ultraviolet B (UVB)-induced pChk1. HeLa cells were pretreated with various concentrations of a test compound for 1 h. Cells were then rinsed with PBS and either sham-treated (N: no UV) or irradiated with UVB. Cells were again incubated with the relevant compound for 1 h prior to harvest.

(**D**) Summary of numbers of small molecules of interest following screens.

(**E**) Chemical structures of novel ATR pathway inhibitors and caffeine. Concentrations at which compounds inhibited HU-induced pChk1 to the same level of inhibition by 3 mM caffeine are shown. The concentrations were obtained using data shown in **Figure 2A**.

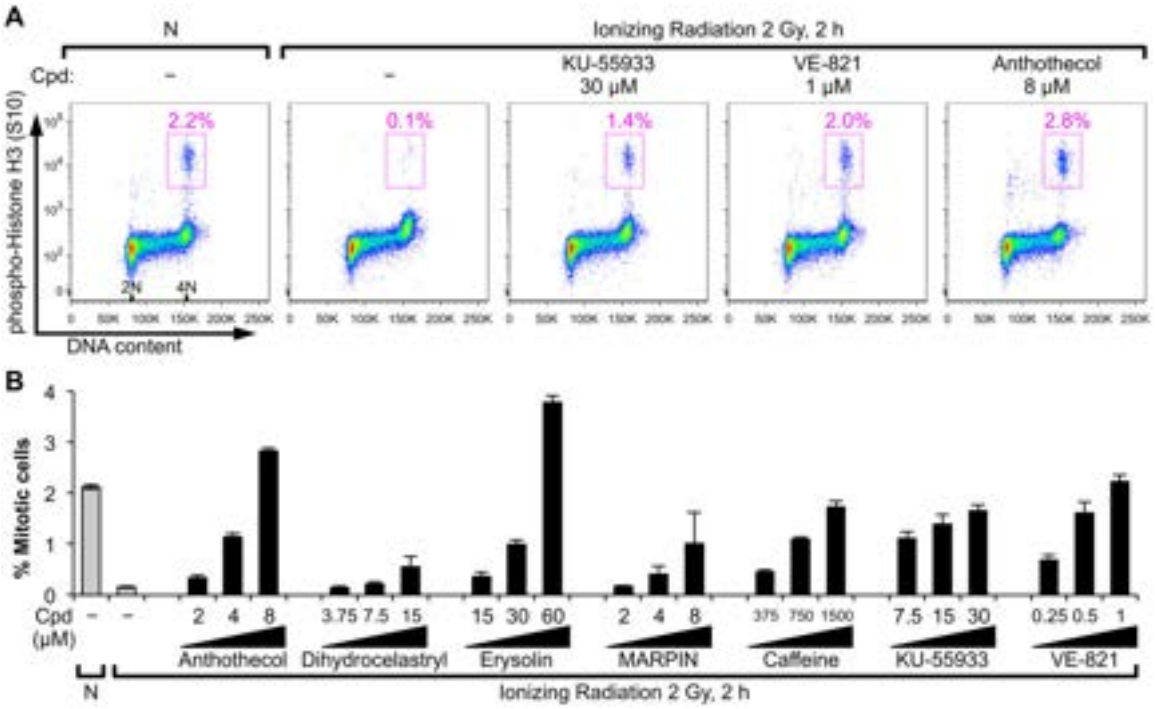

Figure 3. Novel ATR pathway inhibitors abrogate G_2/M checkpoint induced by ionizing radiation in a dose-dependent manner

HCT116 $p53^{+/+}$ cells were pretreated with a test compound (Cpd) for 30 min. Cells were then treated with 2 Gy of ionizing radiation (IR) or mock treated (N: no IR). After 2 h, cells were harvested, fixed, and stained with anti-phospho-Histone H3 (Ser10) antibody and FxCycle Violet (DNA content) for flow cytometry analysis.

(**A**) Representative flow cytometry plots are shown. Mitotic cells (pink boxes) are defined as cells positive for phospho-Histone H3 (Ser10) with 4N DNA content. Percentage of mitotic cells is indicated above each pink box.

(**B**) Effects of novel ATR pathway inhibitors and known ATM/ATR inhibitors on IR-induced G_2/M checkpoint were evaluated as percentage of mitotic cells. Two-fold serial dilutions of compounds were tested. Mean of percentage of mitotic cells is shown (n = 3). Error bars indicate standard error of the mean.

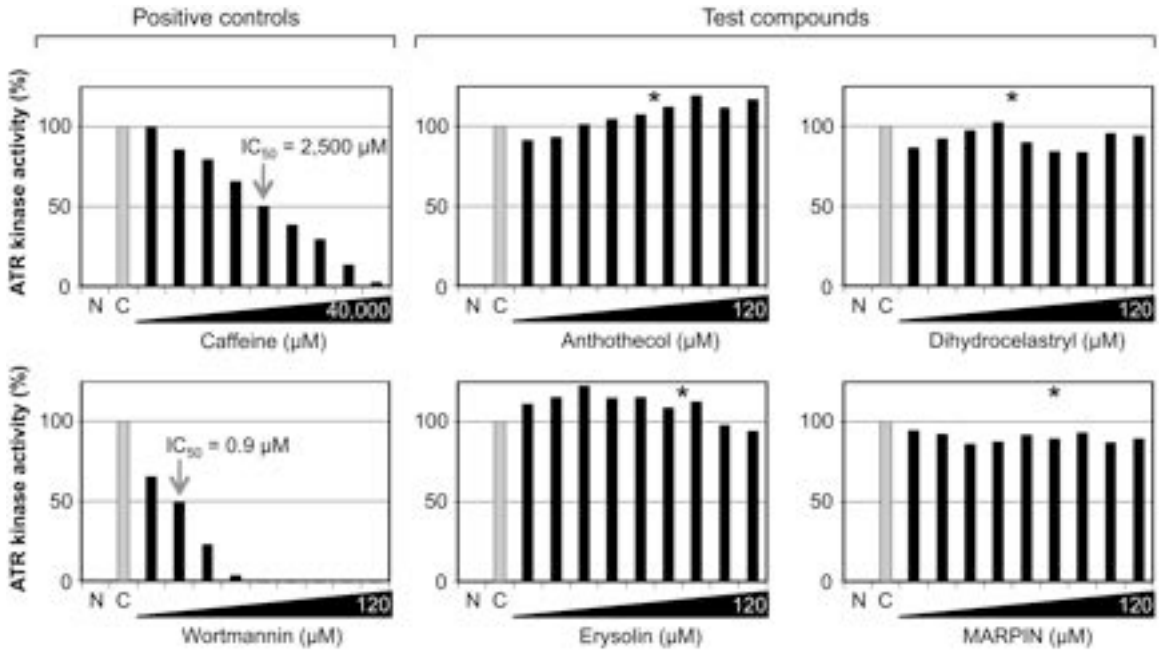

Figure 4. Novel ATR pathway inhibitors do not inhibit *in vitro* ATR kinase catalytic activity

ATR kinase activity was measured by incorporation of radioactive phosphate into a peptide substrate. Immunopurified ATR proteins were mixed with [γ-^{32}P]ATP, a Rad17-derived peptide as substrate, and the indicated concentrations of compounds or DMSO (vehicle). Two-fold serial dilutions of compounds were tested in triplicate, and mean of ATR kinase activity is shown. The highest concentration (μM) used for a compound is indicated within the black triangles. ATR kinase activities were normalized by subtracting background signals seen in samples with no substrate (N) and setting DMSO vehicle control with substrate (C) to 100% (grey bar). Arrows indicate IC_{50} values determined by this ATR kinase assay. Asterisks indicate the concentrations of these novel compounds that were required in cell-based assays (Fig. 2A) to inhibit hydroxyurea-induced phosphorylation of Chk1 with the same potency as 3 mM caffeine.

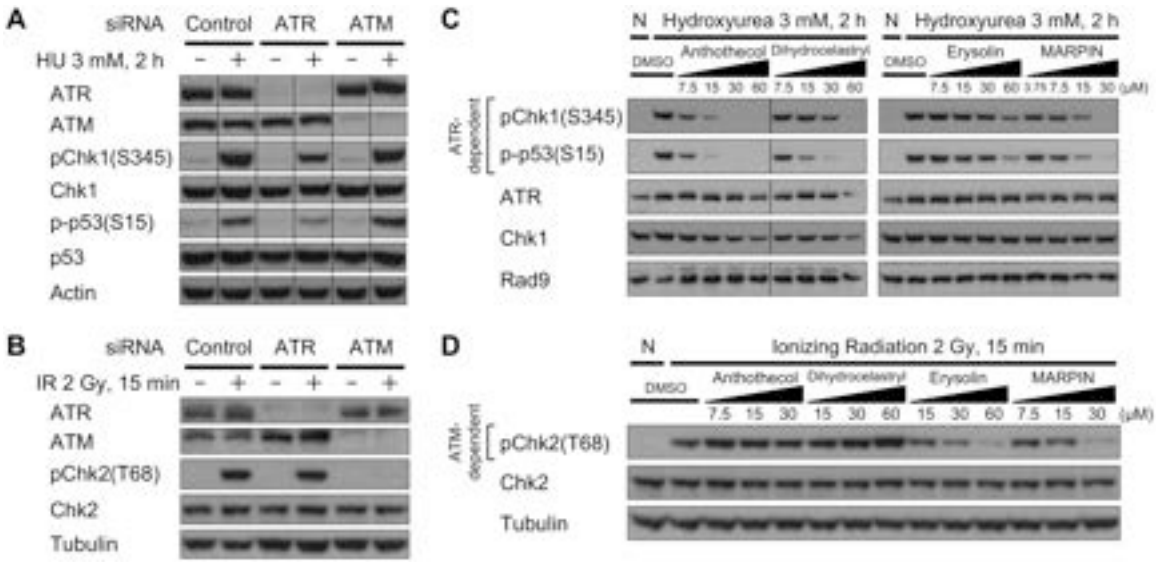

Figure 5. All four novel compounds inhibit ATR signaling; erysolin and MARPIN also suppress ATM signaling at an early time point

(**A**) ATR-selective phosphorylation of Chk1 and p53 following hydroxyurea (HU). 293T cells were transfected with scrambled siRNA (control) or siRNA against ATR or ATM. 48 h after transfection, cells were treated with or without 3 mM HU for 2 h. Clarified cell lysates were used for Western blot analyses with the indicated antibodies.

(**B**) ATM-selective phosphorylation of Chk2 following ionizing radiation (IR). HCT116 $p53^{+/+}$ cells were transfected with siRNA. 48 h after transfection, cells were treated with 2 Gy of IR and harvested 15 min later. Clarified cell lysates were subjected to Western blot analyses with the indicated antibodies.

(**C**) Inhibition of ATR-selective phosphorylation by four compounds. 293T cells were mock treated (N: no HU) or treated with 3 mM HU and various concentrations of compounds for 2 h. DMSO was used as vehicle. Two-fold serial dilutions of compounds were tested. ATR, Chk1, and Rad9 were used as loading controls.

(**D**) Inhibition of ATM-selective phosphorylation by two compounds. HCT116 $p53^{+/+}$ cells were pretreated with various concentrations of compounds for 30 min, followed by 2 Gy of ionizing radiation (IR) or mock treatment (N: no IR). Cells were harvested 15 min after IR. Two-fold serial dilutions of compounds were tested. Chk2 and Tubulin were used as loading controls.

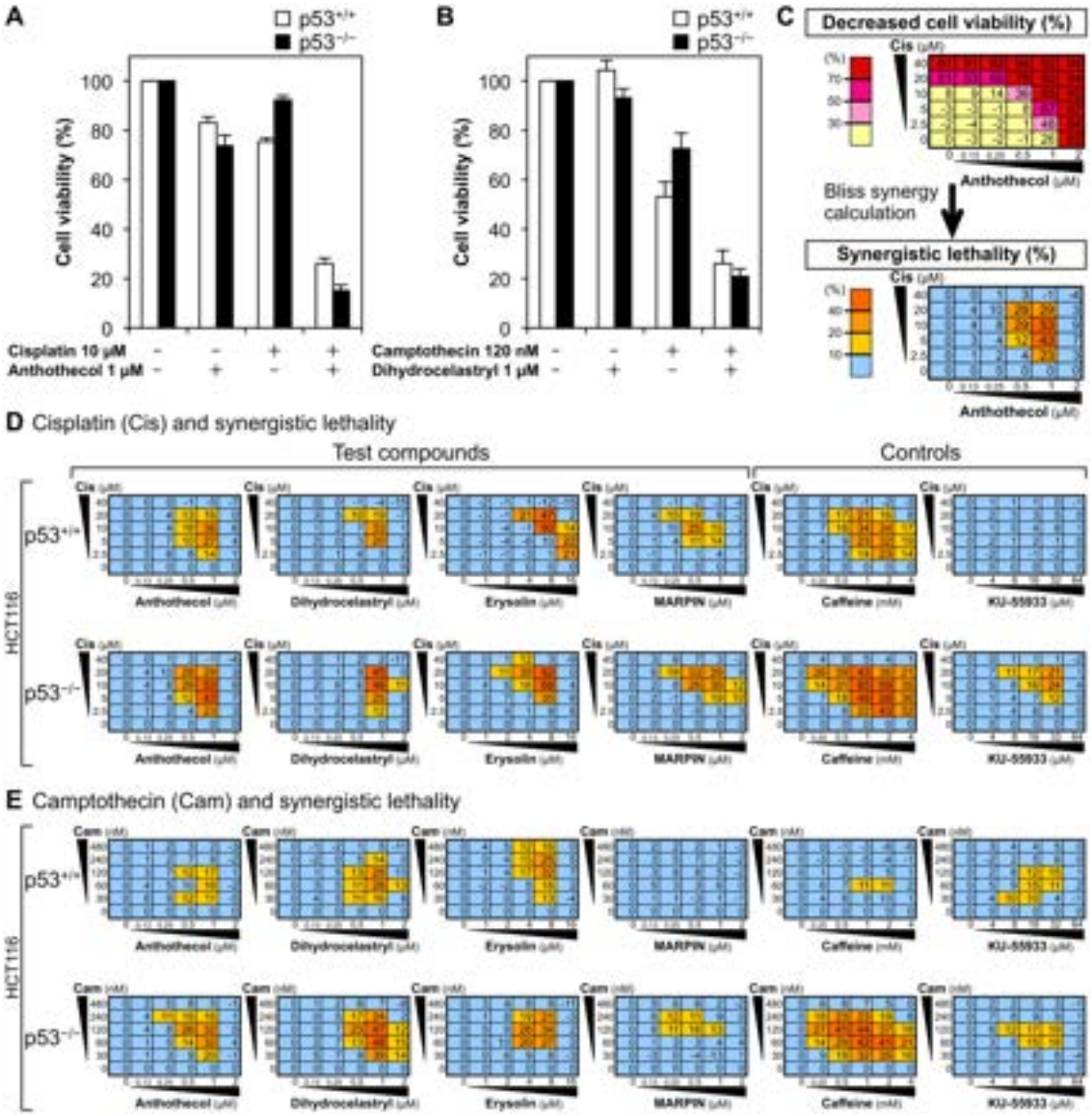

Figure 6. Novel ATR pathway inhibitors sensitize p53-deficient cancer cells to DNA-damaging agents *in vitro*

(**A**) Sensitization of p53-deficient cells to cisplatin by a novel ATR pathway inhibitor, anthothecol. HCT116 $p53^{+/+}$ cells and the isogenic $p53^{-/-}$ cells were treated with cisplatin and/or anthothecol for 48 h. Cell viability was measured using a colorimetric metabolic assay (WST-8). Cell viability of mock treated cells was set to 100%, and mean of cell viability is shown ($n = 4$). Error bars indicate standard error of the mean.

(**B**) Sensitization of p53-deficient cells to camptothecin by a novel ATR pathway inhibitor, dihydrocelastryl. Cell viability after 48 h incubation with compounds was measured as in **Figure 6A**.

(**C**) Representative data of decreased cell viability and calculated synergistic lethality. A combination of cisplatin and anthothecol in HCT116 $p53^{-/-}$ cells is shown. Decreased cell viability (%) was calculated by subtracting % cell viability from 100% and is shown for each pair of compound combinations in a dose matrix using a color scale. Darker red

indicates stronger decrease in cell viability. Excess over Bliss additivism was used to calculate synergistic effects of compounds on decreased viability as described in Supplementary Methods. The calculated synergistic lethality (%) is shown in a dose matrix using a different color scale. Darker orange indicates higher synergistic lethality, meaning that a combination of two compounds (a DNA-damaging agent and an ATR pathway inhibitor) synergistically decreased cell viability.

(**D & E**) Synergistic effects on decreased cell viability in various combinations of DNA-damaging agents (cisplatin (**D**) or camptothecin (**E**)) and ATR pathway inhibitors in HCT116 $p53^{+/+}$ and $p53^{-/-}$ cells. Cell viability after 48 h incubation with compounds was measured as in **Figure 6A**, and synergistic lethality was calculated using cell viability data shown in Supplementary Figure S1. The calculated synergistic lethality (%) is shown in dose matrices using the same color scale as in lower panel of **Figure 6C**. Caffeine served as a positive control ATM/ATR inhibitor. KU-55933 was used as an ATM-specific inhibitor.

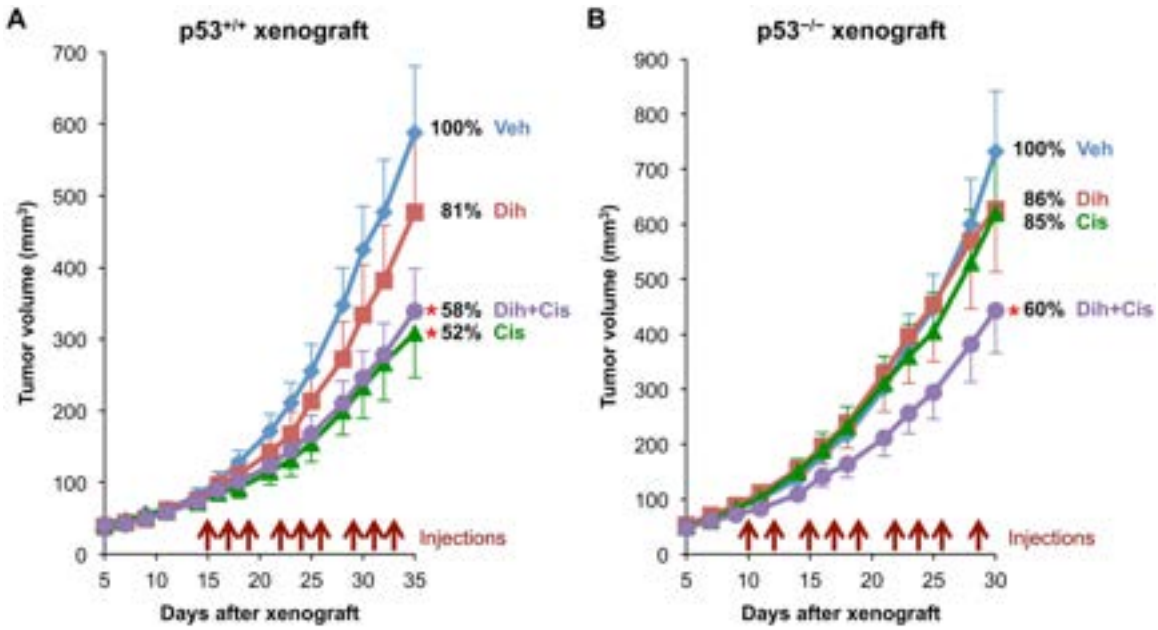

Figure 7. A novel ATR pathway inhibitor synergistically suppresses p53-deficient tumor growth when combined with cisplatin in a xenograft model

HCT116 $p53^{+/+}$ (**A**) or HCT116 $p53^{-/-}$ cells (**B**) (5×10^6 cells/mouse) were subcutaneously injected into the right flank of athymic nude mice (10-17 weeks old). After mean volume of tumors in all mice exceeded 75 mm^3, mice were randomly divided into 4 treatment groups, and compounds were intraperitoneally injected 3 times per week for 3 weeks (total 9 injections; brown arrows). In each drug treatment, 0.12% DMSO in PBS (vehicle) or dihydrocelastryl (Dih) 0.1 mg/kg/day was injected initially, followed 30 min later by PBS (vehicle) or cisplatin (Cis) 2 mg/kg/day as indicated. Tumor volume was measured by a caliper 3 times per week. Mean of tumor volume in each treatment group is shown. Error bars indicate standard error of the mean ($n = 10$ for all four treatment groups for $p53^{+/+}$ xenografts; $n = 11$ for the Dih treatment group for $p53^{-/-}$ xenograft; $n = 12$ for the other 3 treatment groups for $p53^{-/-}$ xenografts). Final tumor sizes (volumes) after 9 injections were compared with vehicle treatment group (Veh) and were shown as % control. Asterisks indicate statistical significance of the final tumor volumes compared with vehicle treatment group ($P < 0.05$).